

AIR TRAFFIC SIMULATION ACROSS FIR IN JAPAN USING CELLULAR AUTOMATON

Katsuhiko Sekine¹, Tomoaki Tatsukawa¹, Kozo Fujii¹ & Eri Itoh^{2,3}

¹Tokyo University of Science

²The University of Tokyo

³Electronic Navigation Research Institute

Abstract

A large-scale air traffic simulation is performed by using cellular automaton (CA)-based model with high fidelity and simple rules. Air traffic flow has become complicated due to the recent increase in global air traffic, resulting in daily operational delays. Therefore, our simulation focuses on large-scale traffic flow rather than specific airspace to design an operation system achieving both the safety and efficiency of the entire air traffic management (ATM). In this study, every 4934-aircraft flying across Flight Information Region (FIR) in Japan, called Fukuoka FIR, is simulated by extending the analysis area of our previous CA-based model, which estimates delay time and the bottleneck by the interaction between in-trail aircraft. Our CA-based model can represent air traffic flow including operational rules, aircraft characteristics, and weather conditions, which the macroscopic model cannot easily take into consideration. Furthermore, our model is fairly simple to set up compared to multiagent-based simulation, which belong to the same meso/microscopic model. As a result, the macroscale analysis clarifies that the spacing adjustments of arrival flights to the hub airports account for only 40% of the total amount. This indicates that identifying flight delay bottleneck not only on the airways to hub airports but also on other routes is also paramount for totally efficient ATM operation.

Keywords: air traffic flow, air traffic management, cellular automaton (CA)-based model, large-scale simulation

1. Introduction

Air traffic demand is expected to recover in the next four years despite the sharp reduction due to COVID-19, albeit with uncertainty [1]. This increasing demand has caused air traffic flow to concentrate in specific airspace and time zones with the consequence of the imbalance between demand and capacity. With the demand exceeding capacity, aircrafts before take-off will be queued at the airport of origin, whereas in-flight aircraft will be instructed to bypass the congested airspace. In addition to the above air traffic flow management (ATFM), especially around large-scale congested airports, aircraft will be path-stretched by "Vectoring" and stacked by "Holding" to keep the assigned separation at the runway threshold, which complicate air traffic flow. These cumulative delays lead not only to a decrease in customer satisfaction, but also to an increase in fuel consumption, adversely affecting the environment. The ratio of delays by air traffic flow has become large for the past decades; e.g., such a delay was reported to 30% of the total in EU in 2010 [2]. Therefore, reducing the delay originating from air traffic flow is increasingly becoming a vital factor in air traffic management (ATM).

Air traffic flow has been modeled and simulated focusing on large-scale areas in order to clarify the mechanism of delay propagation and consequently predict the delay. Macroscopic models are commonly used for large-scale simulations by approximating the flow of aircraft by continua and calculating macro variables (e.g., traffic volume, density, and average velocity). However, such a model cannot necessarily explain the air traffic flow, affected by complex operational rules and

weather conditions. In contrast, meso/microscopic models, such as cellular automaton (CA)-based and multiagent-based models, calculate the microvariables (e.g. position, velocity) of each aircraft through the interaction between aircraft (or aircraft groups). Although multiagent-based models can describe phenomena in detail, the parameters are apt to become large in number, which requires time and effort for the rule-setting. CA-based models develop the behavior of the entire system based on the interaction between each agent, allowing one to reduce the number of parameters. However, most CA-based models in the past have tended to focus on specific airspace, mainly used to investigate better conflict resolution.

This paper performs a large-scale air traffic simulation to design an operation system that achieves both safety and efficiency of the entire air traffic management (ATM). Here, a CA-based model is used to effortlessly model large-scale air traffic flows with high fidelity. In this study, every 4934 aircraft that fly across the Flight Information Region (FIR) in Japan, called Fukuoka FIR, is simulated by extending the analysis area of our previous CA-based model. This paper is organized as follows. Section 2. summarized the related work to model air traffic flow. Section 3 describes the overview of CA-based simulator. Section 4. compares the simulation results to actual track data to generate trust in our proposed CA-based model. Section 5 discusses the results obtained.

2. Literature Review

Air traffic flow has previously been simulated in demand capacity balance (DCB) studies, congestion analysis, and other ATM-related studies, using mathematical models such as queue [3, 4, 5, 6], the differential equation [7, 8, 9, 10, 11, 12], and network [13, 14, 15, 16]. Many strategic ATM concepts based on these models have been proposed, and these concepts enable a low computational cost. However, mathematical and theoretical models are not necessarily able to explain air traffic flow precisely because they are based on several complex rules and are strongly affected by aircraft facilities and weather. Multiagent-based modeling is a different approach that has also been utilized in the field of ATM by several researchers [17, 18, 19, 20, 21]. Although multiagent-based models can describe phenomena in detail, it is difficult to develop a highly accurate model because of the high degree of freedom required. The cellular automaton model is similar to the multiagent-based model, but is simpler. A cellular automaton model (CA) is a discrete computational model that consists of a regular grid of cells, with each cell existing in one of the finite numbers of states, such as 0 and 1. The state of each cell is updated after each discrete time interval in accordance with simple rules. As mentioned by Sun et al. [22], the cellular automaton model is computationally friendly compared to the Eulerian flow theory and the PDE models, which are theoretical models.

Several CA models[23, 24, 25, 26, 27, 28, 29] have been proposed to analyze air traffic flow. Kim et al. [23] proposed a two-dimensional CA model to demonstrate an airborne self-separation system by describing aircraft that move in all directions within adjacent airspaces. Yu et al. [24] and He et al. [25] utilized a one-dimensional CA model that can simulate the aircraft landing process to schedule the aircraft landing time in real time. Wang et al. [26] and Lim et al. [27] adopted a two-dimensional CA model for en-route airspace by combining optimization techniques to find flight paths that avoid prohibited airspace, restricted airspace and dangerous airspace. Enayatollahi et al. [28, 29] constructed a two-dimensional CA model considering a standard terminal arrival route (STAR) to investigate the impact of weather on delays and to optimize the flight path following performance-based navigation (PBN). Most studies have not focused on constructing a CA model in global airspace, such as Japan and Europe, but in terminal airspace or specific en-route airspace.

To address this gap, we have proposed a one-dimensional CA model with step back movement (SBCA) that was constructed considering Tokyo International Airport (RJTT) [30] and Japan [31]. Our objective was to contribute to the production of a set of fast-time simulation and optimization tools in which ATM stakeholders can quickly and easily change airspace and routes to verify new ATM concepts. Therefore, the unique characteristics of SBCA is its ability to model air traffic flow with

only a few parameters, simple input files, and simpler rules than those followed in previous related studies.

3. Cellular Automaton (CA)-based models

A one-dimensional CA model with Step-Back movement (hereafter, SBCA) is used to simulate air traffic flow. Our proposed CA-based approach was already used to simulate inflow traffic at Tokyo International Airport (RJTT) modeled in the terminal airspace of Tokyo International Airport (RJTT), so-called Tokyo Approach Control Area (TACA) [30], and in Japan [32]. Our previous work focuses not only on modeling the air traffic flow but also optimizing take-off time [31] and cruise speed [33] of arrival track at RJTT to obtain knowledge contributing to efficient ATM operation. In [33], the decision tree was used to extract the optimal speed control strategy from the optimization results. This study extends the modeling area to FIR in Japan, the so-called Fukuoka FIR, and simulates the behavior of all 4934-flights through their interactions as shown in Figure 1.

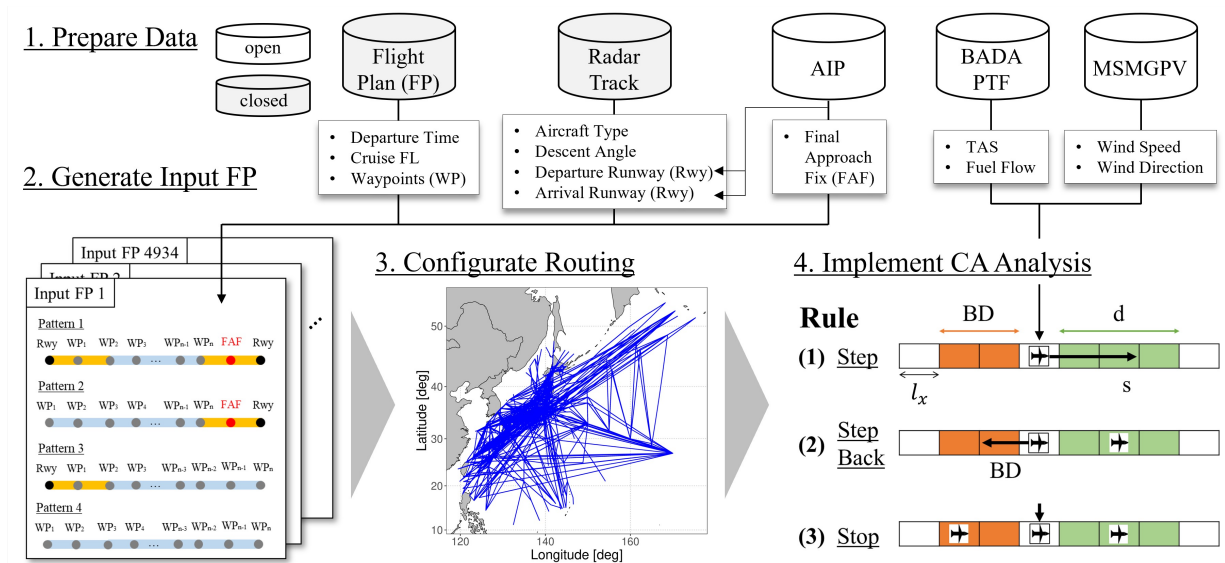


Figure 1 – Designing a CA-based model in large-scale analysis area

3.1 Data Preparation

3.1.1 Flight Plan

A flight plan (FP) is a plan that notifies the air traffic control agency when an aircraft flies. FPs are not open to the public, and are provided by the Civil Aviation Bureau in Japan (JCAB). A FP includes the call sign, aircraft type, the name of captain, flight rules, departure fix, departure time, cruise altitude, route, cruise speed, radio equipment, alternative airport, fuel load, total number of passengers, and other information. SBCA utilizes departure time at the first row of a FP, maximum cruise flight level (FL), and route with the name of waypoints (WP) including latitude and longitude. Once the aircraft leaves the reference point, it follows exactly the designated flight path until arrival.

3.1.2 Radar Track

Radar track is the time series trajectory data created from the actual data and the flight plan data from the radar information processing system for air traffic control. In Japan, the radar track from 2012 to 2017 is open to the public as CARATS Open Data [34] provided by JCAB. However, Tokyo International Airport (RJTT), the hub airport for domestic flights, has just started the new sequencing and spacing operation, so-called point-merge (PM) operation, since 2019, which changes the characteristics of the air traffic flow. Therefore, the radar track from 2019 to 2020, closed data provided

by JCAB, is used to input the data into SBCA.

The radar tracks include the time recorded by approximately 10 seconds, the call sign, the latitude, longitude, the altitude and the type of aircraft. From the above data, call sign, aircraft type, departure runway, arrival runway, and descent angle from the top of descend to runway threshold are extracted. The arrival / departure runways are estimated using the nearest-neighbor algorithm by comparing the first and last rows of the radar track for each flight with the runway threshold location of the departure / arrival airport extracted from the Aeronautical Information Publication.

3.1.3 Aeronautical Information Publication

Aeronautical Information Publication (AIP) [35] is a national publication that contains permanent information necessary for the operation of air traffic control. Permanent changes to the recorded content will be made by the revised version of AIP, whereas temporary changes will be made by the supplementary version of AIP. Aeronautical Information Publication (AIP) consists of three parts: General Rules (GEN), Enroute (ENR), and Airfield (AD), each of which is appropriately divided into sections containing various information items. The entire AIP is divided into 5 volumes, the first volume is GEN and ENR, and the second and subsequent volumes are AD. The "General Rules (GEN)" contain rules which include national rules and requirements, tables and symbols, operations, airfield / heliport use, and navigational assistance fees. Above the AIP, the location of runway thresholds of all domestic airports and the final fix approach (FAF) are extracted.

3.1.4 Base of Aircraft Data

The BADA model is a model that allows calculations such as aircraft movement and fuel consumption using aircraft data provided free of charge by the European Organization for the Safety of Air Navigation (EUROCONTROL) [36]. Aircraft specifications (e.g., aerodynamic coefficient, mass, wing area, and fuel consumption required for CL and CD calculation) required for four-dimensional trajectory prediction and fuel consumption estimation are summarized in a data file for each model. As of 2020, three types, BADA Family3, BADA Family4, and BADA Family H, have been released. BADA Family H is a helicopter-specific model. BADA Family4 provides more accurate aircraft specification data than Family3, nevertheless the use of the model is limited. The BADA Family3 covers the specification data for all models flying in EU controlled areas and even includes unmanned aerial vehicles (RPAS) flying on remotely controlled aircraft systems (RPAS) such as Global Hawk and Predator, therefore, used in SBCA. For simplification, the Performance Table File (PTF), which describes the performance during ascent, cruising, and descent at each flight level for a specific type of aircraft following the BADA Family3, is used to calculate the trajectory.

3.1.5 Meso Scale Model Grid Point Value

MesoScale Model Grid Point Value (MSMGPV) [37] provided by the Japan Meteorological Agency is used as a model for wind speed and direction. The main purpose of this model is to predict phenomena that cause disasters, such as heavy rains and storms, several hours to a day ahead, with a horizontal grid spacing of 5 km and the calculation area of Japan and the sea nearby. Forecasts are made 8 times a day, every 3 hours, and up to 39 hours in advance. The latitude is 22.4 degrees north latitude to 47.6 degrees north latitude with 253 vertical grids at 0.1 degree intervals, and the longitude is 120 degrees east longitude to 150 degrees east longitude with 241 horizontal grids at 0.125 degree intervals. Regarding the area out of the above zones, the nearest point is used instead. Since there are 16 barometric pressure planes from 100 [hPa] to 1000 [hPa], there are a total of 975568 lattices. Atmospheric pressure is calculated in advance and temperature and atmospheric density at each altitude are calculated using the BADA model and formulas in the standard atmosphere and are used to calculate the behavior of the aircraft.

3.2 Input Flight Plan and Routing

Figure 2 illustrates the pattern of the input flight plan. The route constructed by waypoints is segmented into two zones according to the flying area because the in-trail separation is around 3 to 5 NM inside terminal control airspace around domestic airports compared to more than 5 NM outside terminal airspace, called en-route airspace. In this study, these zones are defined as the "Terminal Control Segment (yellow zone)" and the "En-Route Segment (blue zone)", respectively, for the parameter setting mentioned in Section 3.4 Combining the information mentioned in Section 3.1 the pattern of the input flight plans are divided into four categories. "Pattern 1" is for domestic flights, which depart the runway threshold and arrive at the destination runway. "Pattern 2" and "Pattern 3", on the other hand, is the international flights which take off or arrive at the runway threshold in Japan. "Pattern 4" is the flyover, the international flights that do not take off and land at the domestic airports. As a result, by combining all flight plans, the airways are defined as the network shown in Figure 3.

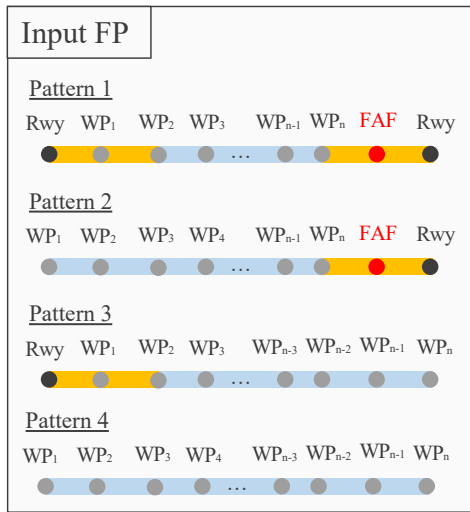


Figure 2 – Pattern of input flight plan (Yellow zone is "Terminal Control Segment" whereas blue zone is "En-Route Segment")

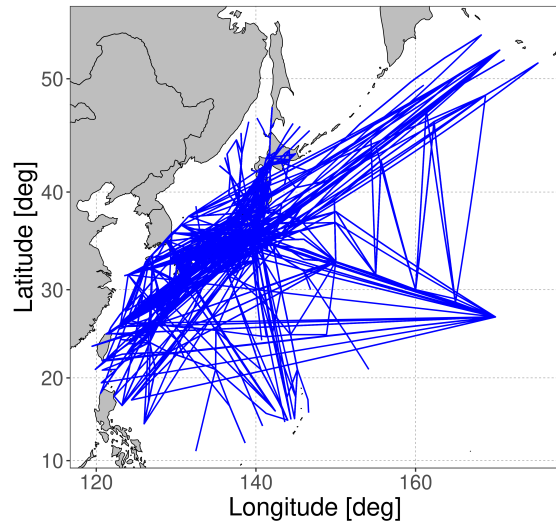


Figure 3 – Airways (blue lines) in Fukuoka FIR in Japan

3.3 Rule Setting

Our rule-based simulator[31] has been improved to take into account not only arrivals but also departures. In [31], arrival traffic to Tokyo International Airport (RJTT), the most congested airport in Japan, has been simulated by the three simple rules. In this study, the runway crossing rules is added to consider the interaction on the runway.

3.3.1 Basic Rule

As shown in Figure 4, SBCA consists of 3 basic rules that utilize 2 parameters, d and BD , and aircraft speed s . d is the minimum in-trail separation between aircraft, and BD is the step-back distance. A velocity s is assigned to each aircraft, calculated using Base of Aircraft Data (BADA) and Meso Scale Model Grid Point Value (MSMGPV). In Rule 1, when there is no aircraft in the front for a distance of d , then the aircraft moves forward by s (Step). In Rule 2, when there is one or more aircraft in the front within a distance of d , and there is no aircraft in the rear for a distance of BD , the aircraft moves backward by BD (Step Back). In Rule 3, when there are one or more aircraft in the front within a distance of d and in the rear within a distance of BD , then the aircraft remains in its current position (Stop). "Step Back" and "Stop" correspond to spacing adjustments, such as "Holding" and "Vectoring".

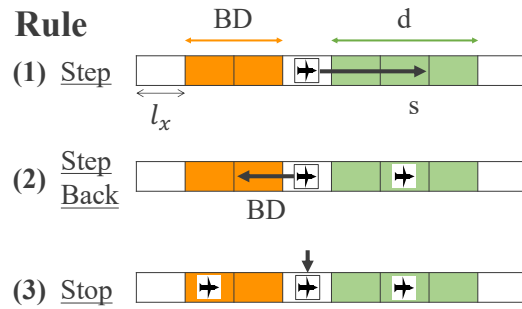


Figure 4 – Analysis area

3.3.2 Runway Interaction Rule

Figure 5 illustrates the runway interaction rule. As mentioned in [38], there are three factors to limit the maximum runway capacity, namely, wake turbulence categories, safety margins, and runway occupancy time (ROT). In this study, wake turbulence categories is considered, which means safety margin and ground movements such as landing roll and taxiing are excluded. The runway interaction is modeled by used two parameters, d_{stop} and T . d_{stop} is the parameter to keep the departure aircraft waiting at the runway threshold, while T is the parameter to update the start time for the departure aircraft. As illustrated in Fig. 5, when the landing aircraft, Arr , approaches at distance d_{stop} , the departure aircraft, dep_{next} , is stopped at the runway threshold. Once Arr lands at the runway threshold, dep_{next} can take off in T to maintain separation. This parameter T is also used to update the take-off time for the departure and departure pairs. In this way, this runway crossing rule prioritizes to make the arrival aircraft land at the runway threshold as soon as possible, representing the real-world operation.

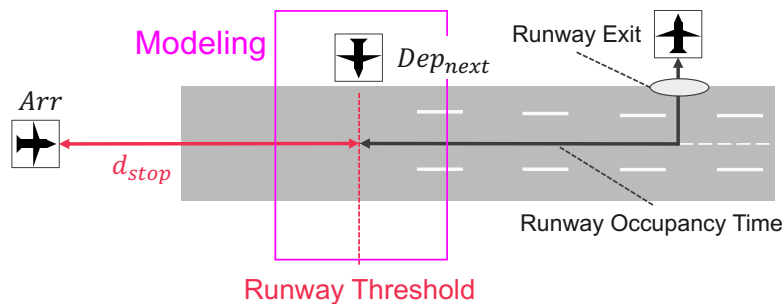


Figure 5 – Runway interaction rule

3.4 Parameter Setting

All parameters of SBCA are defined based on a data-driven analysis of flight plans (FP), radar track data and publication of aeronautical information (AIP). One of the most significant features is that the parameters d and BD are set as simple as possible. The parameters for basic rules is shown in Table 1. Basically, d is 7NM and 4NM in Enroute and Terminal section defined in blue and yellow zones in Fig. 2, respectively. At the final approach fixes (FAFs) extracted from AIP, d is defined as the sum of the wake turbulence distance separation minima (WTDSM) and buffer (2NM) to consider the safety margin.

The parameters for the basic rules are shown in Table 2. These parameters are derived from our previous study using AirTOP simulator [39], which is a fast-time simulation platform based on multi-agent models that enable gate-to-gate simulation of air traffic [38]. d_{stop} is set to 3.5NM, which is the default value of the runway dependency parameter, while T is set to the minimums of separation of the time of turbulence after awakening (WTTSM).

Table 1 – Parameter Setting for Basic Rules

Parameter	Value
l_x	70 [m]
Δt	1 [s]
Enroute	7 [NM] / ($l_x/1852$)
d Terminal	4 [NM] / ($l_x/1852$)
FAF	WTDSM + 2 [NM] / ($l_x/1852$)
BD	0 [NM]

Table 2 – Parameter Setting for Runway Interaction Rule

Parameter	Value
d_{stop}	3.5 [NM]
T	WTTSM [s]

4. Analyzing Proposed CA-based model

Our preliminary results obtained from a single nominal day simulation show that SBCA captures well the characteristics of actual air traffic flow. As shown in Figure 6, the spacing adjustments of Rule 2 and 3 (magenta points) are proactively implemented in the southwest vicinity of RJTT, the domestic hub airport in Japan, as reported in our previous studies, exclusively simulating arrival traffic to RJTT [31]. Interestingly, these spacing adjustments are extensively implemented across the Fukuoka FIR due to the interaction of each aircraft. Regarding the number of spacing adjustments, Table 3 summarizes the statistical analysis of the top 10 destinations of the total number (S_{adj}). The description of each columns are as follows:

N_{arr} The number of arrivals at each destination runway threshold.

S_{adj} The total number of spacing adjustments implemented by the flights to the destination.

CCR_{adj} The cumulative ratio of the S_{adj} .

$N_{arr,adj}$ The number of the flights implementing the spacing adjustments in N_{arr} .

E_{adj} The averaged value of S_{adj} .

M_{adj} The median value of S_{adj} .

σ_{adj} The standard deviation of S_{adj} .

Min_{adj} The minimum value of the number of spacing adjustments of the flights to the target destination.

Max_{adj} The maximum value of the number of spacing adjustments of the flights to the target destination.

In addition to RJTT, RJAA is the hub airport for international flights. Significantly, counting the number of magenta points in Fig. 6 quantitatively reveals that the number of spacing adjustments for arrival flights to RJTT and RJAA represents only 40% of the total number (= 333,364) according to Table 3. Even including these hub airports, the number of spacing adjustments for flights arriving at the destination shown in Table 3 covers 80% of the total number. The eight airports shown in Table 3 are known as the main airports in Japan. These results indicate that identifying the flight delay bottleneck not only on the airways to major airports, but also on other routes, is paramount for a totally efficient ATM operation.

Airways on the Pacific Ocean, however, is colored magenta as shown in Figure 6, though the flights on those routes fly linearly in the actual operation. The main cause of the discrepancy is a consequence of the modeling using one-dimensional CA, in which the aircraft always follows the in-trail separation. In the actual operation on the Pacific Ocean, the flights on the same Flight Level (FL) band are separated by 50 NM while the flights on the different FL band do not separated laterally. In the simulation, the in-trail separation is set 7 NM, approximately one-seventh of the actual, but the passing of aircrafts each other does not occur on those routes, which would be the source of the

AIR TRAFFIC SIMULATION ACROSS FIR IN JAPAN USING CELLULAR AUTOMATON

spacing adjustments. However, the discrepancy are considered as insignificant due to the fact that the magenta plots on the Pacific Ocean are faded out, meaning that the spacing adjustments are not actively implemented compared to those on the islands of Japan.

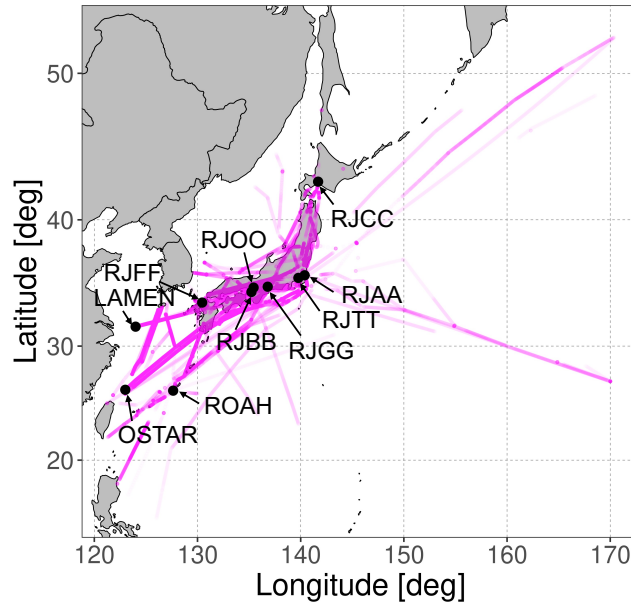


Figure 6 – Projection of the position of the spacing adjustments by Rule 2 and 3 (pink plot). The deeper in color the plot is, the more congested it is.

Table 3 – Summary of the spacing adjustments by Rule 2 and 3

Destination	Category	Airport Type	Runway threshold	N_{arr}	S_{adj}	CCR_{adj}	$N_{arr,adj}$	E_{adj}	M_{adj}	σ_{adj}	Min_{adj}	Max_{adj}
RJTT	Airport	Hub airport	34L 34R	472 154	66353	0.200	409	162.23227	123.0	127.832793	1	759
RJAA	Airport	Hub airport	34R 34L	329 38	63560	0.392	251	253.22709	148.0	295.612125	3	1754
ROAH	Airport	Major airport	36	178	24375	0.466	94	259.30851	124.0	371.446693	5	1564
RJOO	Airport	Major airport	32L 32R	179 0	22550	0.534	107	210.74766	106.0	262.236682	3	1386
RJBB	Airport	Major airport	06L 06R	253 19	22082	0.600	143	154.41958	97.0	183.927933	1	1085
LAMEN	Waypoint	-	-	214	15410	0.647	91	169.34066	109.0	174.131254	1	888
RJFF	Airport	Major airport	34	232	14824	0.692	115	128.90435	88.0	122.983380	1	536
OSTAR	Waypoint	-	-	168	12855	0.730	72	178.54167	118.5	185.796264	1	793
RJCC	Airport	Major airport	01L 19R	191 15	12605	0.768	95	132.68421	121.0	97.876960	3	418
RJGG	Airport	Major airport	18	158	9208	0.796	66	139.51515	103.5	144.782409	1	663

Further analysis reveals that the trends of the number of adjustments vary according to the destinations. Figure 7 shows the dispersion of the number of the spacing adjustments according to each destination shown in Table 3. The range between Min_{adj} and Max_{adj} is about 700 in the case of RJTT, the destination of the largest number of spacing adjustments. On the other hands, these range in RJAA, ROAH, RJOO and RJBB has longer tail of the number over 1,000. This result suggests that these airports have a local peak of the congested time period when flights are kept waiting in the air. Besides the above macroscale analysis, investigating meso-microscale flow behavior (e.g., inflow of the hub airports) generates trust in SBCA.

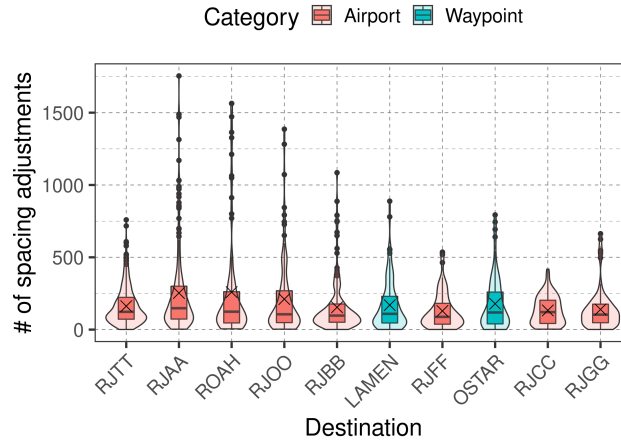


Figure 7 – Boxplot of the number of spacing adjustments by Rule 2 and 3 per flight

Figure 8 compares the dominant inbound tracks at RJTT and RJAA depicted both upstream (between 250NM and 80NM from the destination) and downstream airspace (within 80NM centered at the destination), where the path stretching by 'Vectoring' is actively implemented. These figures explain that the positions where Rule 2 and 3 are applied (magenta points) are generally fitted to where the actual tracks (blue lines) are largely deviated away from the FPs (black lines) due to 'Vectoring'.

Figure 9 shows the error rate ($ER[\%] = (D_{sim} - D_{act})/D_{act} \times 100$) calculated for each flight within the upstream airspace (ER_{up} , red boxplot) and downstream airspace (ER_{down} , blue boxplot). The result shows that 50% of ER_{up} falls within the range between $\pm 5\%$ at all target destinations. Furthermore, half of ER_{down} excluding RJFF34, ROAH36 and RJGG18 ranges roughly from -10% to $+10\%$, although aircrafts adjust their spacing more frequently. These results suggest that even simple rules could represent the phenomenon of spacing adjustment for arrival traffic flow. On the contrary, ER_{down} of RJFF34, ROAH36, and RJGG18, which are used as arrival and departure, show greater variation compared to the other runway thresholds. A reasonable explanation for this is that the runway interaction rule adopted in the simulation prioritizes arrival flights. In case the demand in the number of departures is extremely high, the arrivals are kept waiting in the vicinity of the airport, thereby stretching the traveling distance in the actual record. In such a case, the separation is controlled by the distance with a few buffers larger than the wake-turbulence separation minima. The rule does not fully represent the air traffic controllers' task, especially sequencing the arrival and departure flights, thus there is certainly room for improvement.

Figure 11 compares the travel distance between the concentric circles every 10 NM depicted in Figure 10. Importantly, beyond 60 NM, the mean, median, and interquartile range of the traveling distance of the simulation agree with that of the actual data. Combining the error rate of the traveling distance, in our view, the result further emphasizes the validity of our model. In contrast, the larger gap between the simulation data and the actual data occurs within 50 NM. Conceivably, this gap at RJTT, which is one of the example of arrival-only runway threshold, can be explained by the constraints of the location of the spacing adjustments. For example, the final approach fix (FAF) is

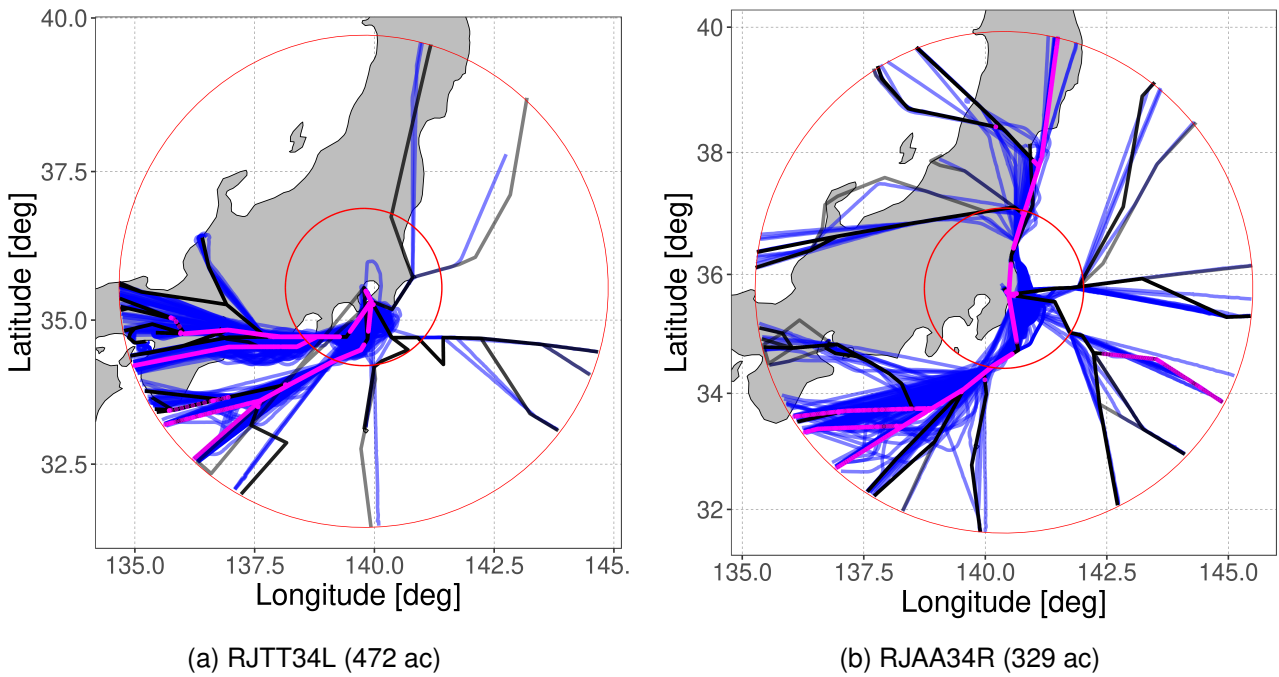


Figure 8 – Comparison between actual in-bound tracks (blue lines) and simulation in-bound tracks (black lines) with the positions of the spacing adjustments by Rule 2 and 3 (magenta points) depicted within 250NM (outer red circle) and 80NM (inner red circle) centered at the destination

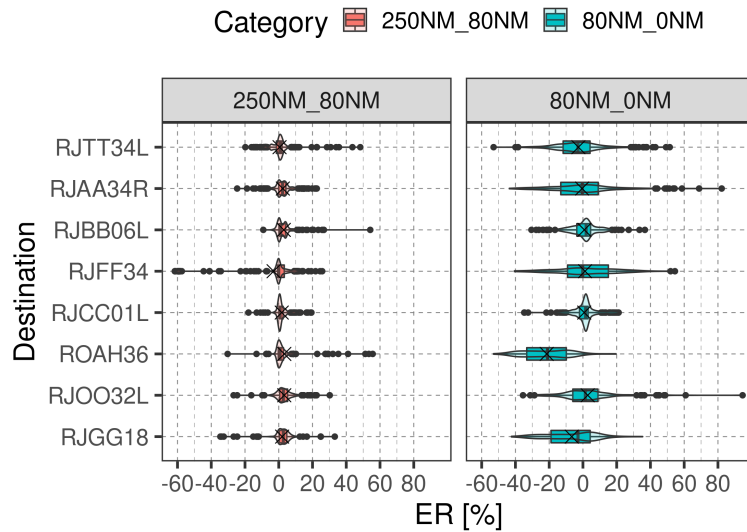


Figure 9 – Boxplot with estimated probability density function of simulation error-rate of traveling distance based on actual track in between concentric circles

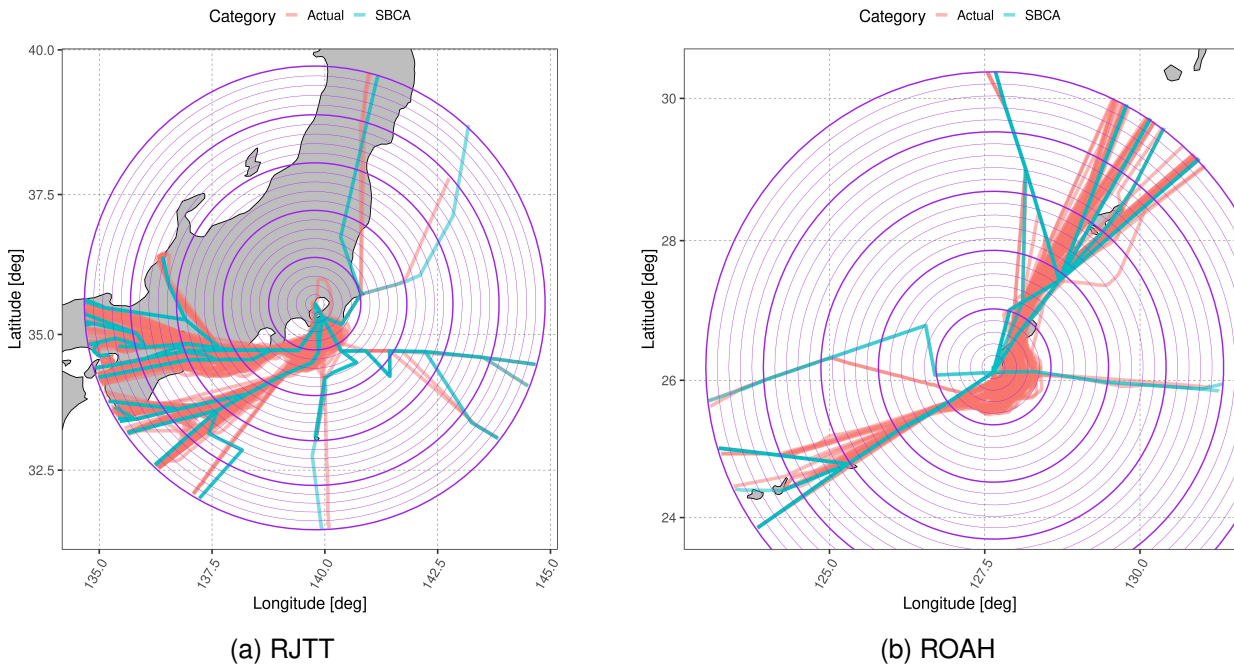


Figure 10 – Comparison between actual in-bound tracks (red lines) and simulation in-bound tracks (blue lines). Concentric circles (purple lines) are depicted at every 10 NM radi

located approximately 20 NM away from RJTT, where the flights that go ahead anyway are actively separated in the simulation, thereby traveling distance at 20 NM in SBCA (blue boxplot) has the peak as shown in Fig. 11a. On the other hand, "Vectoring" is actively implemented several tens of NMs before FAF following AIP [35], which justifies that the traveling distance at 50 NM in the actual data (red boxplot) is the largest in mean and median. Regarding ROAH, which is one of the examples of runway arrival-departure thresholds, the parameters d and BD affect the gap between the simulation and the actual operation, as well as the simplicity of the runway crossing rule. d at FAF of every runway threshold is set assuming a wake turbulence separation, often implemented at hub airports. However, the separation values vary depending on the target airports, which in part accounts for the difference between the simulation and the actual operation. Moreover, such a separation value is often uniformly set with the considerable amount of buffer because of the safety concerns about the interaction of the arrival and the departure. Especially for ROAH, attention to ship and vessel below flights with the phase of approach is unable to disregard. These factors are possible explanation for the gap of the traveling distance occurring at the runway threshold used as departure and arrival combination. In addition to the traveling distance, the inter-aircraft time (IAT) at the runway threshold reflects similar trends.

Figure 12 demonstrates the IAT at RJTT34L and ROAH36. Note that the ROAH36 distribution has both arrival and departure data. As shown in Figure 12a, the peak of the distribution is found to be in harmony with the actual data at RJTT34L, the runway threshold for arrival only. This result indicates that the runway arrival operation in the simulation capture well the characteristic of the actual operation as the result of the spacing adjustments. On the other hand, the peak IAT at ROAH36 obtained from the simulation does not fit to the actual value as depicted in Figure 12b. As mentioned in Figure 9, the runway interaction rule used in the simulation does not completely represent the actual operation of the arrival and departure runways at which wake turbulence separation is not implemented. Furthermore, arrival flights on the course to ROAH36 are concerned about the ship and vessel, which could be one of the factor of increasing IAT.

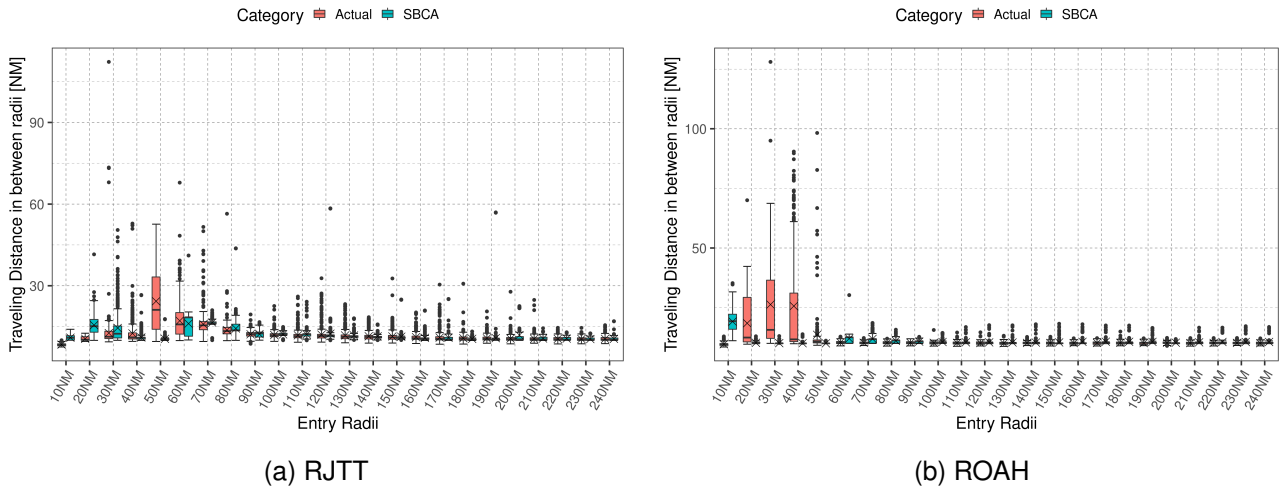


Figure 11 – Comparison between actual traveling distance (red boxplot) and traveling distance obtained in the simulation (blue boxplot). The metric is defined by the traveling distance between the concentric circles of radi r NM and $r - 10$ NM ($r \in 10, 20, \dots, 240$) depicted in Fig. 10.

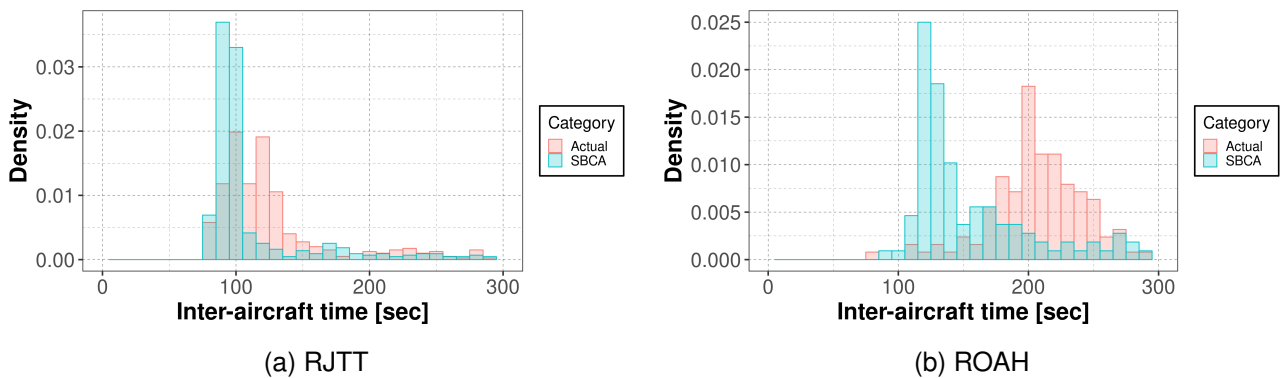


Figure 12 – Comparison between actual in-bound tracks (blue lines) and simulation in-bound tracks (black lines) with inter-aircraft time

5. Discussion

This study simulated the one-day track in Fukuoka FIR by extending the analysis area in our previous study, which proposed a model based on a cellular automaton (CA). Our CA-based model represented spacing adjustments by using three basic rules and a runway interaction rule, taking into account the characteristic of aircraft, the operational constraints and weather conditions.

The most notable result that emerges from the simulation is that the spacing adjustments originated from the hub airports, RJTT and RJAA, only represented approximately 40% of the total as shown in Table 3. Despite including the other major airports in Japan, the number of spacing adjustments were less than 80% of the total. This finding seems to imply that air traffic management, such as speed control and departure metering, for not only the hub and major airports but also other destinations, is key to reducing airborne delays. Given the peak of traveling distance in Fig 11, the source of the delay times was found to come from the vicinity of the airport, where the sequencing and spacing of the flights is actively implemented. Furthermore, the dispersion of the spacing adjustments vary according to the destinations (see Figure 7). The results point to the probability that the air traffic management considering the target area and time period would contribute to efficient operation. As a result, these spacing adjustments extended traveling distance, worth utilizing to validate our model. Excluding the outliers in Figure 11, half of ER_{up} and ER_{down} fell in the range between $\pm 5\%$ and $\pm 10\%$, respectively, at the arrival-only runway thresholds in the major airports in Japan. This result indicates that our CA-based model captures well the characteristics of arrival traffic flow, which is more complex than departure traffic flow due to spacing adjustments, in spite of only adopting simple parameter setting.

Although our CA-based model is advantageous in quantifying the airborne delay bottleneck in a large area, one-dimensional modeling in which the flights are not considered vertically separated restricts the application of the operation. As shown in Figure 4, the spacing adjustments (magenta plots) occurred on the Pacific Ocean though the aircraft flying there did not actually implement path-stretching, resulting in the overestimation of the spacing adjustments. Moreover, focusing on the destination used as both arrival and departure, disagreement of the traveling distance around the destination and the peak of the distribution of the inter-aircraft time (IAT) at the runway threshold is evident (see Figure 11b and Figure 12b). There are several sources of possible errors. First, the parameters d and BD were set globally (see Table 1) following our previous work [31]. Especially, considering the wake turbulence separation at FAF of every runway threshold would become the factor to increase the error, possibly underestimating the number of spacing adjustments. Second, since the focus of the runway interaction rule was on runway thresholds, the variance of the IAT did not fit completely to that of the actual data, including the impact of runway occupancy time (see Figure 12). Thus, to improve delay estimation accuracy, our future work will apply multilayer lanes in the altitude direction in part, investigate the influence of changing the parameters in our model, and collaborate with the model simulating the surface operation.

6. Concluding Remarks

A large-scale simulation by using a simple air traffic model which adjusts the space of aircraft using one-dimensional CA has been described. 4934 aircraft flying in Fukuoka Flight Information Region (FIR) were simulated using the actual flight plan, the actual radar track, the aeronautical publication information, Base of Aircraft DATA (BADA), and Meso Scale Model Grid Point Value (MSMGPV). Improving our previous CA-based model with step back and stop rules which add the flight distance corresponding delay time, the runway interaction rule was implemented to consider delay time originating from runways, which are the bottleneck of air traffic management. As a result of fixing the distance parameter required for approaching arrival d_{stop} and the time parameter for wake turbulence separation minima T , the number of spacing adjustments of the flights toward the hub airport, RJTT and RJAA, only made up 40% of the total. The finding of this study supports the idea that arrival

traffic to local airports as well as hub airports is paramount for totally efficient air traffic management (ATM). Our approach could be applied to other large-scale FIR with the simple parameter setting and high fidelity, clarifying the bottleneck of delay time accordingly.

To further our research, we are currently planning to implement co-simulation taking the surface operation into account including the important delay factors (e.g., runway occupancy time, runway crossing, runway exit locations, taxiing routes and spot assignment). Coupling en-route and ground models proposed by our research group will enable us to quantify the overall delay time through the gate-to-gate simulation in a large-scale analysis area. Furthermore, future work will investigate the air traffic flow on the Pacific Ocean to clarify whether rules for overtaking is necessary for our CA-based model. Controlling air traffic flow (e.g. departure metering and speed control) in our model, the aim of this research will be to propose the best strategies for designing global-optimal and robust ATM systems from a broader perspective toward post-pandemic.

Acknowledgement

This research was carried out with the support of the JSPS Grant-in-Aid for Scientific Research, KAKENHI, No. 20H04237 in Japan. In addition, the traffic flow simulator used in this study was developed in the research project of “Exploratory Challenge 2 (ID : hp190163) on Post-K computer” (Construction of Models for Interaction Among Multiple Socioeconomic Phenomena, sub-issue: Model Development and Applications for Enabling Robust and Optimized Social Transportation Systems). Finally, we appreciate the data and technical support from the Civil Aviation Bureau.

References

- [1] International Air Transport Association (IATA). Five years to return to the pre-pandemic level of passenger demand. *International Air Transport Association*, 2019.
- [2] EUROCONTROL. Network operations report for 2010, 2010.
- [3] Richard M Harris. Models for runway capacity analysis. Technical report, MITRE CORP MCLEAN VA, 1972.
- [4] Milan Janić and Vojin Tošić. Terminal airspace capacity model. *Transportation Research Part A: General*, 16(4):253–260, 1982.
- [5] Mark Hansen. Micro-level analysis of airport delay externalities using deterministic queuing models: a case study. *Journal of Air Transport Management*, 8(2):73–87, 2002.
- [6] Nikolas Pyrgiotis, Kerry M Malone, and Amedeo Odoni. Modelling delay propagation within an airport network. *Transportation Research Part C: Emerging Technologies*, 27:60–75, 2013.
- [7] Padmanabhan K Menon, Gregory D Sweriduk, and Karl D Bilimoria. New approach for modeling, analysis, and control of air traffic flow. *Journal of guidance, control, and dynamics*, 27(5):737–744, 2004.
- [8] PK Menon, GD Sweriduk, T Lam, GM Diaz, and Karl D Bilimoria. Computer-aided eulerian air traffic flow modeling and predictive control. *Journal of Guidance, Control, and Dynamics*, 29(1):12–19, 2006.
- [9] Daniel B Work and Alexandre M Bayen. Convex formulations of air traffic flow optimization problems. *Proceedings of the IEEE*, 96(12):2096–2112, 2008.
- [10] Dengfeng Sun and Alexandre M Bayen. Multicommodity eulerian-lagrangian large-capacity cell transmission model for en route traffic. *Journal of guidance, control, and dynamics*, 31(3):616–628, 2008.
- [11] P Wei, Y Cao, and D Sun. Total unimodularity and decomposition method for large-scale air traffic cell transmission model. *Transportation Research Part B: Methodological*, 53:1–16, 2013.
- [12] Honghai Zhang, Yan Xu, Lei Yang, and Hao Liu. Macroscopic model and simulation analysis of air traffic flow in airport terminal area. *Discrete Dynamics in Nature and society*, 2014, 2014.
- [13] Takahiro Ezaki and Katsuhiko Nishinari. Potential global jamming transition in aviation networks. *Physical Review E*, 90(2):022807, 2014.
- [14] Dan Chen, Minghua Hu, Yuanyuan Ma, and Jianan Yin. A network-based dynamic air traffic flow model for short-term en route traffic prediction. *Journal of Advanced Transportation*, 50(8):2174–2192, 2016.
- [15] K.K.H. Ng, C.K.M. Lee, Felix T.S. Chan, Chun-Hsien Chen, and Yichen Qin. A two-stage robust optimisation for terminal traffic flow problem. *Applied Soft Computing*, 89:106048, 2020.
- [16] Kam K.H. Ng, Chun-Hsien Chen, and C.K.M. Lee. Mathematical programming formulations for robust airside terminal traffic flow optimisation problem. *Computers & Industrial Engineering*, 154:107119, 2021.

- [17] Sameer Alam, Hussein A Abbass, and Michael Barlow. Atoms: Air traffic operations and management simulator. *IEEE Transactions on intelligent transportation systems*, 9(2):209–225, 2008.
- [18] David Šišlák, Přemysl Volf, and Michal Pěchouček. Agent-based cooperative decentralized airplane-collision avoidance. *IEEE Transactions on Intelligent Transportation Systems*, 12(1):36–46, 2010.
- [19] Adrian K Agogino and Kagan Tumer. A multiagent approach to managing air traffic flow. *Autonomous Agents and Multi-Agent Systems*, 24(1):1–25, 2012.
- [20] Yash Guleria, Qing Cai, Sameer Alam, and Lishuai Li. A multi-agent approach for reactionary delay prediction of flights. *IEEE Access*, 7:181565–181579, 2019.
- [21] Alessandro Pellegrini, Pierangelo Di Sanzo, Beatrice Bevilacqua, Gabriella Duca, Domenico Pascarella, Roberto Palumbo, Juan José Ramos, Miquel Àngel Piera, and Gabriella Gigante. Simulation-based evolutionary optimization of air traffic management. *IEEE Access*, 8:161551–161570, 2020.
- [22] Dengfeng Sun, Issam S Strub, and Alexandre M Bayen. Comparison of the performance of four eulerian network flow models for strategic air traffic management. *Networks & Heterogeneous Media*, 2(4):569, 2007.
- [23] Charles Kim, K Abubaker, and Obinna Obah. Cellular automata modeling of en route and arrival self-spacing for autonomous aircrafts. In *50th Annual Meeting of Air Traffic Controllers Association*, pages 127–134, 2005.
- [24] Sheng-Peng Yu, Xian-Bin Cao, and Jun Zhang. A real-time schedule method for aircraft landing scheduling problem based on cellular automation. *Applied Soft Computing*, 11(4):3485–3493, 2011.
- [25] Yueshuai He, Kaiquan Cai, Yongliang Li, and Mingming Xiao. An improved cellular-automaton-based algorithm for real-time aircraft landing scheduling. In *2014 Seventh International Symposium on Computational Intelligence and Design*, volume 1, pages 284–288. IEEE, 2014.
- [26] Shi jin Wang and Yan hui Gong. Research on air route network nodes optimization with avoiding the three areas. *Safety Science*, 66:9–18, 2014.
- [27] Wen-Xian Lim and Zhao-Wei Zhong. Re-planning of flight routes avoiding convective weather and the “three areas”. *IEEE Transactions on Intelligent Transportation Systems*, 19(3):868–877, 2017.
- [28] Fatemeh Enayatollahi and MA Amiri Atashgah. Wind effect analysis on air traffic congestion in terminal area via cellular automata. *Aviation*, 22(3):102–114, 2018.
- [29] Fatemeh Enayatollahi, MA Amiri Atashgah, SM Malaek, and Parimala Thulasiraman. Pbn-based time-optimal terminal air traffic control using cellular automata. *IEEE Transactions on Aerospace and Electronic Systems*, 2021.
- [30] Tomoaki Tatsukawa, Shinsuke Nagaoka, Koya Anzai, and Kozo Fujii. A study of air traffic simulation around haneda airport using step back cellular automaton. In *Proceeding of 2018 AIAA Guidance, Navigation, and Control Conference*, page 1597, 2018.
- [31] Katsuhiro Sekine, Tomoaki Tatsukawa, Eri Itoh, and Kozo Fujii. Multi-objective takeoff time optimization using cellular automaton-based simulator. *IEEE Access*, 9:79461–79476, 2021.
- [32] Katsuhiro Sekine, Tomoaki Tatsukawa, Shinsuke Nagaoka, and Kozo Fujii. Preliminary study of multi-objective air traffic optimization by using step back cellular automaton. In *Proceeding of AIAA Aviation 2019 Forum*, page 3407, 2019.
- [33] Katsuhiro Sekine, Tomoaki Tatsukawa, Kozo Fujii, and Eri Itoh. Extraction of speed-control strategy in en-route air traffic using multi-objective optimization and decision tree. In *Proceeding of AIAA Aviation 2022 Forum (in press)*, 2022.
- [34] Air Navigation Services Department Civil Aviation Bureau, MLIT. Data extracted from the air navigation services department’s database becomes available. <https://www.mlit.go.jp/common/001082594.pdf>, 2015.
- [35] Japan Aeronautical Information Service Center. Aeronautical Information Publication (AIP). <https://aisjapan.mlit.go.jp/>, 2020.
- [36] EUROCONTROL. User manual for the base of aircraft data (bada) revision 3.8. <https://www.eurocontrol.int/publication/user-manual-base-aircraft-data-bada-revision-38>, 2010.
- [37] Research Institute for Sustainable Humanosphere, Kyoto University. Meso-scale model grid point value (mmsgpv). <http://database.rish.kyoto-u.ac.jp/index-e.html>, 2020.
- [38] Katsuhiro Sekine, Furuto Kato, Kota Kageyama, and Eri Itoh. Data-driven simulation for evaluating the impact of lower arrival aircraft separation on available airspace and runway capacity at tokyo international airport. *Aerospace*, 8(6), 2021.
- [39] AirtopSoft. Airtop software. <https://airtopsoft.com/>, 2020.

Copyright Statement

The authors confirm that they, and/or their company or organization, hold copyright on all of the original material included in this paper. The authors also confirm that they have obtained permission, from the copyright holder of any third party material included in this paper, to publish it as part of their paper. The authors confirm that they give permission, or have obtained permission from the copyright holder of this paper, for the publication and distribution of this paper as part of the ICAS proceedings or as individual off-prints from the proceedings.